

SCIENTIFIC REPORTS



OPEN

Weighted Symbolic Dependence Metric (wSDM) for fMRI resting-state connectivity: A multicentric validation for frontotemporal dementia

Sebastian Moguilner^{1,2,3}, Adolfo M. García^{1,4,5}, Ezequiel Mikulan^{1,4}, Eugenia Hesse^{1,4,13}, Indira García-Cordero^{1,4}, Margherita Melloni^{1,4}, Sabrina Cervetto^{1,6}, Cecilia Serrano⁷, Eduar Herrera^{1,4,8}, Pablo Reyes⁹, Diana Matallana⁹, Facundo Manes^{1,4,10}, Agustín Ibáñez^{1,4,10,11,12} & Lucas Sedeño^{1,4}

The search for biomarkers of neurodegenerative diseases via fMRI functional connectivity (FC) research has yielded inconsistent results. Yet, most FC studies are blind to non-linear brain dynamics. To circumvent this limitation, we developed a “weighted Symbolic Dependence Metric” (wSDM) measure. Using symbolic transforms, we factor in local and global temporal features of the BOLD signal to weigh a robust copula-based dependence measure by symbolic similarity, capturing both linear and non-linear associations. We compared this measure with a linear connectivity metric (Pearson’s R) in its capacity to identify patients with behavioral variant frontotemporal dementia (bvFTD) and controls based on resting-state data. We recruited participants from two international centers with different MRI recordings to assess the consistency of our measure across heterogeneous conditions. First, a seed-analysis comparison of the salience network (a specific target of bvFTD) and the default-mode network (as a complementary control) between patients and controls showed that wSDM yields better identification of resting-state networks. Moreover, machine learning analysis revealed that wSDM yielded higher classification accuracy. These results were consistent across centers, highlighting their robustness despite heterogeneous conditions. Our findings underscore the potential of wSDM to assess fMRI-derived FC data, and to identify sensitive biomarkers in bvFTD.

¹Laboratory of Experimental Psychology and Neuroscience (LPEN), Institute of Cognitive and Translational Neuroscience (INCYT), INECO Foundation, Favaloro University, Buenos Aires, Argentina. ²Fundación Escuela de Medicina Nuclear (FUESMEN) and Comisión Nacional de Energía Atómica (CNEA), Buenos Aires, Argentina. ³Instituto Balseiro and Facultad de Ciencias Exactas y Naturales, Universidad Nacional de Cuyo (UNCuyo), Mendoza, Argentina. ⁴National Scientific and Technical Research Council (CONICET), Av. Rivadavia 1917, C1033AAJ, Buenos Aires, Argentina. ⁵Faculty of Education, National University of Cuyo (UNCuyo), Sobremonte 74, C5500, Mendoza, Argentina. ⁶Departamento de Educación Física y Salud, Instituto Superior de Educación Física, Universidad de la República, Montevideo, Uruguay. ⁷Neurología Cognitiva. Hospital Cesar Milstein., Buenos Aires, Argentina. ⁸Universidad Icesi, Departamento de Estudios Psicologicos, Cali, Colombia. ⁹Intellectus Memory and Cognition Center, Aging Institute, Mental Health and Psychiatry Department, Hospital Universitario San Ignacio, Pontificia Universidad Javeriana, Bogotá, Colombia. ¹⁰Centre of Excellence in Cognition and its Disorders, Australian Research Council (ARC), Sydney, Australia. ¹¹Center for Social and Cognitive Neuroscience (CSCN), School of Psychology, Universidad Adolfo Ibáñez, Diagonal Las Torres, 2640, Santiago de Chile, Chile. ¹²Universidad Autónoma del Caribe, Calle 90, No 46-112, C2754, Barranquilla, Colombia. ¹³Instituto de Ingeniería Biomédica, Facultad de Ingeniería, Universidad de Buenos Aires, Ciudad de Buenos Aires, Argentina. Correspondence and requests for materials should be addressed to L.S. (email: lsedeno@ineco.org.ar)

Received: 7 March 2018
Accepted: 13 July 2018
Published online: 25 July 2018

Functional connectivity (FC) research shows that the brain is intrinsically organized via long-range networks^{1–3}, whose alterations could constitute key biomarkers underlying hallmark deficits across neuropsychiatric conditions and, more particularly, neurodegenerative diseases^{4–9}. Yet, the sensitivity and specificity of such disturbances remains controversial^{5,6,10}. In particular, most FC studies on these diseases are based solely on linear correlation measures, such as Pearson's correlation coefficient (R)^{11–13}, which are blind to concomitant non-linear interactions in brain connectivity^{14–17}. To bridge this gap, we developed a novel measure for fMRI data, inspired in a robust non-linear EEG measure called weighted Symbolic Mutual Information (wSMI)¹⁸, and examined whether it surpassed R in discriminating patients with behavioral variant frontotemporal dementia (bvFTD) from healthy controls, all recruited from two international centers.

The coexistence of linear and non-linear interactions in brain connectivity^{16,17,19,20} is exceedingly simplified by the linearity assumption of most FC studies on neuropsychiatric diseases^{4,5,11–13}, which may be better characterized via nonlinear approaches²¹. Previous attempts in this direction, illustrated by fMRI studies based on the mutual information (MI) metric^{13,22}, have failed to provide substantial new information compared to linear FC measures^{14,23}, even in the comparison between healthy controls and neuropsychiatric patients²⁴. This may be so because traditional MI calculations estimate probability density functions via a histogram approach, which proves inadequate for the small number of samples and low temporal resolution of fMRI data²³.

Notwithstanding, more robust findings might be attained through wSMI¹⁸, a measure devised for EEG analysis which identifies non-linear coupling by transforming recorded signals into discrete sets of temporally aligned symbols, according to the time order of the neighboring data points^{18,21,25}. The ensuing value is then multiplied by a given weight to correct for specific EEG artifacts, like volume conduction and dipole effects¹⁸. This approach has been used to assess network connectivity of socio-cognitive processes through intracranial recordings²⁶ and to detect distributed EEG markers of interoception²⁷ and, more crucially, neurodegeneration²⁸. Moreover, discrimination between bvFTD patients and controls via neuropsychological tests improves upon inclusion of (EEG-derived) wSMI results, further highlighting the sensitivity of this measure to tap into neurodegenerative patterns²⁹. Crucially, then, tapping into intrinsic fMRI connectivity with a similar approach may reveal even more robust markers of neurodegeneration.

Yet, weighted symbolic FC measures have not been applied to fMRI data, arguably because of the latter's low temporal resolution. wSMI measures non-linear coupling through a joint probability matrix (i.e. a joint histogram)¹⁸. When considering long time-series, such as those of EEG signals, histograms yield accurate representations of the distributions. However, this is not the case for the sluggish signals obtained through fMRI. To overcome this limitation, here we employed non-parametric rank statistics with statistical copulas^{30,31}. Copula-based dependence measures, such as Schweizer-Wolff's³² and Hoeffding's Phi-Square³³ metrics, capture both linear and non-linear dependences, even if hidden in uniform background noise³⁴. These measures resemble MI in that they are positive-definite and their value is zero if, and only if, the two measured time-series are independent, and larger values of those copula-dependent measures correspond to larger information sharing³⁰. Of note, extant applications of copulas have been restricted to MEG and EEG recordings, under parametric assumptions²⁴. Moreover, a full and reliable picture of brain connectivity also needs to consider that resting-state networks present transient activity during scan time³⁵, and that the temporal history of the BOLD signal provides useful information for functional connectivity assessment³⁶. Tapping into such intrinsic network connectivity may provide key insights on neurodegeneration³⁷. Thus, to analyze the temporal history pattern of functional connectivity³⁶, we also factored in the time order of neighboring data-points to produce symbols and then calculate a similarity metric between symbolic strings, so that a copula dependence measure can be weighted by symbolic similarity to produce a weighted Symbolic Dependence Metric (wSDM).

To test our approach, we targeted frontotemporal dementia, the second most common neurodegenerative disease in patients below age 65³⁸. Accurate early diagnosis is difficult to achieve in this condition^{38,39}, which undermines household economies and health systems while hindering the development of disease-modifying agents. Although FC measures have emerged as promising biomarkers for this and other neurodegenerative diseases^{5,6,9,10}, their robustness remains inconclusive, with some bvFTD studies showing alterations of the salience network (SN) – a resting-state network encompassing the anterior cingulate cortex (ACC) alongside orbitofrontal and insular regions^{5,6} –, and others showing similar disruptions in Alzheimer's disease (AD)⁶ and other neuropsychiatric disorders⁴⁰. Research on genetic forms of pre-symptomatic bvFTD casts additional doubts, as the SN may be altered⁴¹ or unaltered⁴². Furthermore, SN differences between bvFTD patients and controls, based on seed analysis, prove inconsistent across research centers¹⁰. This high variability and inconsistency, we surmise, might be partially related to the absence of non-linear approaches to fMRI-derived FC data in dementia research^{4–7,9}.

Against this background, the present study evaluated whether the wSDM measure supersedes a linear measure (R) in the identification of resting-state networks and in its capacity to discriminate between bvFTD patients and controls across different recording centers. We collected resting-state fMRI recordings from both populations at two international clinics to assess which measure proved more consistent across centers and their heterogeneous acquisition conditions (e.g., differences in clinical diagnostic groups, fMRI equipment, and acquisition parameters)¹⁰. Then, using seed analysis, we compared results from wSMI and R following two steps. First, we analyzed results from healthy controls to establish which measure proved better at identifying the SN – a well-known resting-state network proposed as a specific FC alteration hallmark of bvFTD^{5,6,43}, the Default Mode Network (DMN) – as a control network that is characteristically affected in other neurodegenerative diseases, such as AD^{5,6,44}, but which has yielded inconsistent results in bvFTD⁶, and a primary sensory (visual) network – that is typically not affected in bvFTD^{5,6}. Second, we compared both methods in terms of their capacity to (i) reveal specific SN differences between patients and controls, and (ii) classify between groups based on FC of the SN using support vector machines (SVM) and nearest neighbor (NN) algorithms. Considering that brain connectivity present both linear and nonlinear components, and that wSMI overcomes relevant limitations of other

	Country-1				Country-2			
	HC	bvFTD	F-values	p-values	HC	bvFTD	F-values	p-values
N	20	20*	—	—	29	15	—	—
Age ^(a)	71.10 (5.16)	73.95 (5.87)	2.65	0.11	61.29 (7.16)	65.94 (7.78)	3.80	0.06
Education ^a	16.72 (3.23)	14.30 (4.57)	2.97	0.09	14.30 (5.67)	14 (4.47)	0.03	0.86
			Chi-square	p-values			Chi-square	p-values
Gender ^b	F = 12	F = 9	0.90	0.34	F = 16	F = 11	1.09	0.29
	M = 8	M = 11			M = 12	M = 4		

Table 1. Demographic details. *Five of the 25 bvFTD patients from Country-1 were discarded after preprocessing; therefore, all reported analyses (including demographic comparisons) were performed only with the remaining 20 participants. ^aANOVA test. Mean (standard deviation). ^bChi-square test. HC: Healthy control. bvFTD: behavioral variant frontotemporal dementia.

measures, we predicted that wSDM would yield more robust results than R in discriminating and classifying between patients and controls.

Materials and Methods

Participants. The study comprised 35 patients fulfilling revised criteria for probable bvFTD⁴⁵ from two international clinical centers with extensive experience in neurodegeneration: the INECO Foundation, from Argentina (Country-1, with 20 controls and 25 bvFTD patients), and the San Ignacio University Hospital, from Colombia (Country-2, with 29 controls and 15 bvFTD patients). As in previous reports from both institutions^{46,47}, clinical diagnosis was established by bvFTD experts (clinical details in Supplementary Information 1). Each sample was matched on gender, age, and education with healthy controls from its respective center (Table 1). All participants provided signed informed consent in accordance with the Declaration of Helsinki. The study protocol was approved by the institutional Ethics Committee of each center (i.e. the INECO Institutional Ethics Committee and the San Ignacio Hospital Ethics Committee).

Image acquisition. Participants from both centers underwent MRI protocols including structural and resting-state sequences. Acquisition and preprocessing steps for each center are reported following the practical guide of the Organization for Human Brain Mapping (OHBM) (see Supplementary information 2 and Supplementary Table 1 for details)^{48,49}.

Preprocessing of fMRI data. Images were preprocessed using the Data Processing Assistant for Resting-State fMRI (DPARSF V.2.3) software⁵⁰ and following previous studies^{10,28,51}. Briefly, the first five volumes were discarded, and then images were slice-time corrected, aligned to the first scan of the session, corrected by nuisance regressions of the white matter and cerebrospinal fluid signals and the six head-motion parameters, normalized to the MNI space, smoothed with an 8-mm full-width half-maximum Gaussian kernel, and finally band-pass filtered (0.01–0.08 Hz). Five bvFTD patients were omitted from Country-1 because of excessive motion (>3 mm/°), yielding the final sample of 20 patients (further details in Supplementary Information 3 and Supplementary Table 2).

Seed analysis. Consistency across controls and differences between groups across countries were explored in the SN and the DMN. We also included a visual network as a complementary control resting-state network that is not typically affected in bvFTD^{5,6}. Seed maps were obtained by using R and wSDM. We placed two bilateral seeds for each network; one pair was located on the posterior cingulate cortex (PCC), a key node of the DMN⁵², other on the dorsal anterior cingulate cortex (dACC), a main hub of the SN⁹, and other on the higher visual cortex⁵³. Seed maps were obtained by using R and wSDM (see details in Supplementary Information 4).

Pearson correlation coefficient. To calculate R, we employed the standard linear correlation function included in MATLAB. We discarded negative correlations –setting them to zero^{10,51,54,55}, because their interpretation is controversial in resting-state studies³.

wSDM. Dependence measures such as MI and wSMI tap into non-linear dependencies yet their application in fMRI studies is limited because of their low temporal resolution⁵⁶. One way to tackle this problem is to use rank statistics, such as in the case of dependency measures based on statistical copulas³⁰. In this way, consider the MI of two random variables x, y :

$$MI(x, y) = \iint f(u^1, u^2) \log \left[\frac{f(u^1, u^2)}{f_1(u^1)f_2(u^2)} \right] du^1 du^2 \quad (1)$$

where f is the joint probability density function (PDF), and f_1, f_2 its marginal PDF. MI is non-negative and it is zero if, and only if, the variables are independent⁵⁷. We can also define MI as a function of the copula, as shown in⁵⁸:

$$MI(x, y) = \iint c(u^1, u^2) \log[c(u^1, u^2)] du^1 du^2 \quad (2)$$

However, this double integral may not have analytical solution.

Let C be the copula function of the random variables (x, y) defined on a unit square. According to Sklar's theorem⁵⁹, there exists a unique copula C that links the joint distribution f and the marginals f_1, f_2 :

$$f(x, y) = C(f_1(x), f_2(y)) \quad (3)$$

Using the result that the variables x, y are independent if and only if the copula C equals the product copula Π defined as the product of their marginal distribution functions³⁰, the independence of the variables can be measured by a normalized L^p distance of C and Π :

$$\left(h_p \iint_{[0,1]^2} |C(u^1, u^2) - \Pi(u^1, u^2)| du^1 du^2 \right)^{\frac{1}{p}}, \quad (4)$$

where $1 \leq p \leq \infty$ and h_p is a normalization constant.

For $p = 1$ and $p = \infty$ we obtain Schweitzer-Wolff's σ and κ , respectively:³²

$$ISW_\sigma = 12 \iint_{[0,1]^2} |C(u^1, u^2) - \Pi(u^1, u^2)| du^1 du^2 \quad (5)$$

and

$$ISW_\kappa = 4 \sup |C(u^1, u^2) - \Pi(u^1, u^2)| \quad (6)$$

where \sup is the supremum under the unit square.

For $p = 2$, we have Hoeffding's phi-square $(I\phi^2)$ ³³,

$$I\phi^2 = 90 \iint_{[0,1]^2} |C(u^1, u^2) - \Pi(u^1, u^2)| du^1 du^2 \quad (7)$$

whose empirical estimation can be analytically computed⁶⁰. We targeted this dependence measure $(I\phi^2)$ because it can be accurately estimated. To calculate it, we employed the Information Theoretical Estimators (ITE) Toolbox⁶¹.

The dependency measure based on statistical copulas^{31,34,56} enables us to estimate MI-like dependence measures despite the low temporal resolution of the fMRI data. However, another limitation of the MI measure (also present in R) is that it overlooks the temporal order of the data points in the time series. Hence, it only provides a static description of FC, thus proving blind to key aspects of neural connectivity^{14,62,63}. However, FC can be also studied by considering the information contained within the BOLD signal's temporal history pattern³⁶. To account for local increases and decreases of the signal, the neighboring values of each time-series data points can be compared to produce symbols via a symbolic transform²¹. Then, we can measure the similarity between two symbol strings considering their respective arrangements to account for time-dependent, global signal modulations.

Let us define a symbolic weight sw which is function of the similarity of \hat{X}, \hat{Y} (i.e., the symbolic transformation of the x, y timeseries). By multiplying the copula-based measure $I(x, y)$ we obtain the formula for the wSDM:

$$wSDM = sw(\hat{X}, \hat{Y}) \cdot I(x, y) \quad (8)$$

The symbolic weights, which range from 0 (i.e., minimal similarity) to 1 (i.e., maximal similarity), were calculated using the Hamming distance⁶⁴ between the obtained symbolic strings. As this index only measures the minimum number of substitutions needed to modify one string to match the other, it is suitable for strings of the same length (e.g., two transformed fMRI time series). Moreover, the Hamming distance is fast to compute in large datasets, such as those comprised of fMRI volumes.

We applied a symbolic transform considering the adjacent neighboring values of each time-series and an output of two possible symbols (i.e., a symbol for the local increase of the signal, and another symbol for the local decrease of the signal). To better understand all the procedures involved in the calculations of the wSDM measure, we have included a flowchart (Supplementary Fig. 1). To evaluate the contribution of the weighted symbols for the dependency measure, we compared our classification results based on the wSDM measures with the ones estimated without applying any symbolic transformation (these results are depicted in Supplementary Table 3 and Supplementary Table 4).

Finally, before we applied the wSDM to the neuroimaging data, we tested it with a simple artificial model to corroborate that it was able to capture non-linear associations (Supplementary Information 5).

Thresholding. We applied a proportional threshold to the association values instead of setting it to a fixed value (e.g. $R = 0.3$) which may bias our results, given that R and wSDM have different units and voxel distributions. By employing different proportional thresholds, we assessed machine learning classification accuracy under different number of features (i.e. number of voxels). To avoid over-fitting when optimizing the threshold hyperparameter, we performed a nested cross-validation using one test set to obtain the optimum threshold and a

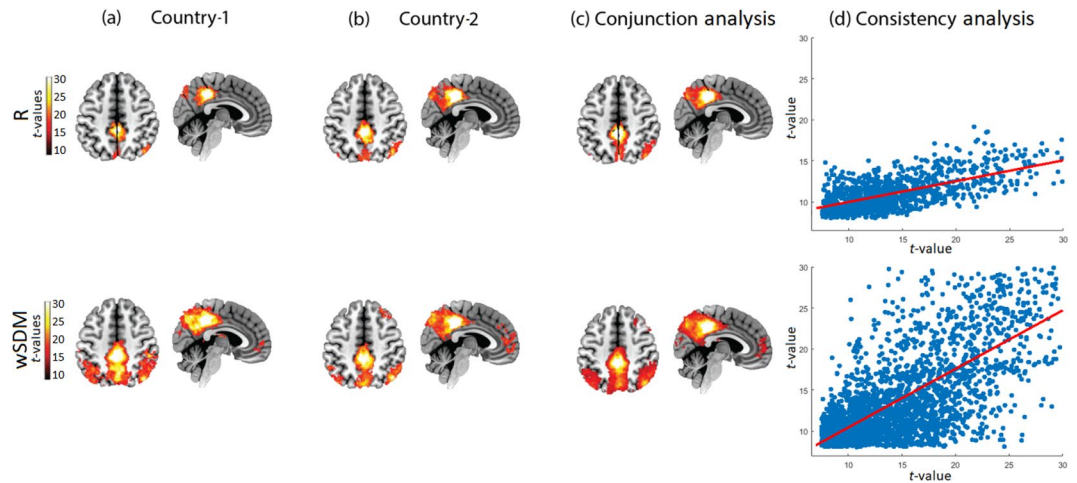


Figure 1. Default mode network (DMN). **(a,b)** Seed analysis results of the DMN using R and wSDM at the 30th percentile threshold, for Country-1 and Country-2 (FWE-corrected, $p = 0.05$ on the voxel level, extent threshold = 30) (axial plane $z = 48$, sagittal plane $x = 4$). **(c)** Cluster overlap between Country-1 and Country-2 (FWE-corrected, $p = 0.05$, extent threshold = 30 voxels). **(d)** Consistency analysis based on a voxel-wise correlation analysis between the maps (T -values) of both countries. All brain images are presented according to neurological convention.

different one to obtain unbiased accuracy rates⁶⁵. Our main results are based on the 30th percentile, which yielded most of the maximum classification accuracy rates on our machine learning analysis, relative to other thresholds (see section 3.3 and Supplementary information 6 for further details). Yet, to show that the seed-based analysis in the control sample resembles previous studies^{66–69} – in which no thresholding approach was applied –, we also report seed results of the DMN and SN in this group without thresholding for both centers (Supplementary Fig. 3 and 4).

Statistical procedures and analysis. To assess the resting-state networks in the control sample of each dataset, we employed a one-sample t -test to display FC of the DMN and the SN (FWE-corrected, $p = 0.05$ at the voxel level, extent threshold = 30 voxels^{70,71}). To evaluate the consistency of these results, we employed a conjunction analysis by overlapping the significant areas across centers (FWE-corrected, $p = 0.05$, extent threshold = 30 voxels)¹⁰. Then, connectivity differences between controls and bvFTD patients were calculated via a two-sample t -test ($p < 0.001$, extent threshold = 30 voxels)^{10,51}. We tested the hypothesis that patients would exhibit hypo-connectivity compared to controls [bvFTD < healthy control] given that it is the most consistently finding about the SN in bvFTD⁶. We applied the same contrast for the DMN: although a few reports have shown increased connectivity of this network in bvFTD^{72,73}, assessments of hypo-connectivity have more consistently revealed null or reduced differences compared to the SN^{42,72–74}. These analyses were run on SPM 12⁷⁵.

To further assess the consistency of seed-analysis findings across countries, we implemented a reproducibility metric used in previous reports^{4,51} (details in Supplementary information 7).

Finally, to identify the most robust association method to discriminate bvFTD patients from controls, we employed both a linear and a non-linear class boundary machine learning classifiers: the SVMs and k-nearest neighbor (kNN) algorithms⁷⁶ (see details Supplementary information 8).

Data availability. The datasets generated during and/or analysed during the current study are available from the corresponding author on reasonable request.

Results

Consistency of resting-state networks in controls. Regarding the DMN, both methods (R and wSDM) evidenced the main posterior regions of this network (i.e., PCC and the angular gyrus); yet, only the latter reproduced the network's anterior section (mPFC) (Fig. 1a,b and Supplementary Table 5). This pattern of results for each method was consistent across countries, as shown by the conjunction analysis (Fig. 1c and Supplementary Table 5). However, the reproducibility metric based on the voxel-wise correlation analysis between the results of each dataset showed higher consistency values for wSDM ($Rho = 0.71$, $p < 0.001$) than for R ($Rho = 0.25$, $p < 0.001$) (Fig. 1d). High correlation values ($Rho > 0.2$, $p < 0.001$) indicate a large consistency of results between datasets, while low values ($Rho < 0.2$, $p > 0.05$) suggest that differences between samples were not consistent across countries⁴. In addition, the slope analysis of the reproducibility metric between measures showed that wSDM yielded significantly different correlation values compared to R (t -value = 31.11, $p < 0.001$). The same pattern was yielded by the analysis of the visual network, with the wSDM presenting higher consistency values across centers (see Supplementary Fig. 8 and Supplementary Table 5).

As regards the SN, both R and wSDM reproduced the main anterior regions of this network (ACC); yet, only the latter included the insula and the fronto-temporal operculum (Fig. 2a,b and Supplementary Table 5). This pattern of results for each method was consistent across countries as shown by the conjunction analysis (Fig. 2c

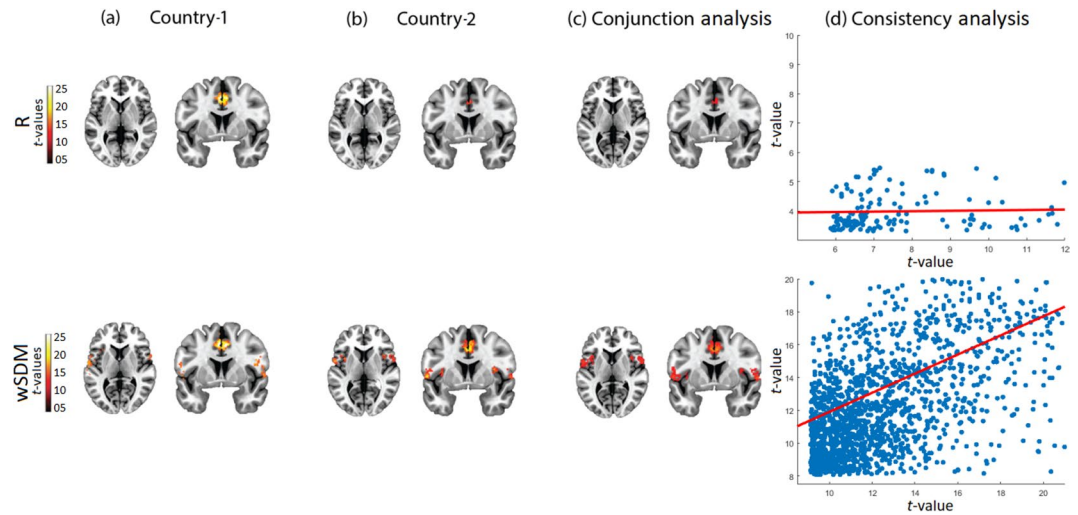


Figure 2. Saliency network (SN). **(a,b)** Seed analysis results of the SN using R and wSDM at the 30th percentile threshold, for Country-1 and Country-2. (FWE-corrected, $p = 0.05$ on the voxel level, extent threshold = 30) (axial plane $z = 3$, coronal plane $y = 6$). **(c)** Cluster overlap between Country-1 and Country-2 (FWE-corrected, $p = 0.05$, extent threshold = 30 voxels). **(d)** Consistency analysis based on a voxel-wise correlation analysis between the maps (T-values) of both countries. The scale of the axis is not the same between methods given the differences in T-values (data dispersion from the R method would not be well illustrated if identical scales were used for each metric). All brain images are presented according to neurological convention.

and Supplementary Table 5). However, the reproducibility metric based on the voxel-wise correlation analysis (Fig. 2d) between the results of each dataset showed higher consistency values for wSDM ($Rho = 0.58$, $p < 0.001$) than for R ($Rho = 0.013$, $p = 0.54$). Moreover, the non-linear measure presented a significantly different slope of association compared to the linear one (t -value = 21.58, $p < 0.001$).

Finally, we also tested the consistency of the extension of the seed-based maps at the individual level, for each method. We found that, relative to R, wSDM presented a more significant homogeneous extension of the DMN and the SN across healthy controls in both centers. As expected, the same was true for patients, but only for the DMN; instead, the SN presented more heterogeneous results, which is consistent with the alteration of this network in bvFTD^{5,6} (for further details, see Supplementary Information 9).

Functional connectivity differences between bvFTD and healthy controls. To evaluate which method was the more powerful to detect connectivity differences between controls and bvFTD patients across centers, we employed two-sample t -tests. Figure 3 shows the connectivity differences after applying the healthy controls > bvFTD contrast for the SN (see also and Supplementary Table 5).

Results from the R method showed a similar pattern of reduced connectivity of the SN in bvFTD for both datasets (Fig. 3: bilateral insular cortex, left fronto-temporal operculum, and left ACC for Country-1; left insular cortex, left fronto-temporal operculum, and right ACC for Country-2). With the wSDM method we also found differences in the main hubs of the SN between groups, but these were larger and covered a greater extension than the ones from R (Fig. 3: bilateral insular cortex and fronto-temporal operculum, and left ACC for Country-1; bilateral insular cortex and fronto-temporal operculum, and right ACC for Country-2). The reproducibility metric based on the voxel-wise correlation analysis between the results of each dataset (as performed above for the analysis of networks only in the control sample) showed higher consistency values for wSDM ($Rho = 0.45$, $p < 0.001$) than for R ($Rho = 0.04$, $p = 0.06$). This difference was further supported by the significant higher slope of the non-linear measure compared to the linear one (t -value = 5.68, $p < 0.001$).

To evaluate the specificity of the SN results, we also compared the DMN and the visual network between patients and controls across centers. None of the methods showed consistent differences between samples, and both presented low reproducibility values across centers (see Fig. 4 for the DMN, and Supplementary Fig. 9 for the visual network). As expected, this suggests that SN alterations may represent a specific (and more consistent than DMN) hallmark for bvFTD.

Machine learning analysis. To evaluate which connectivity method was more accurate to classify bvFTD patients from controls, first we employed the same SVM classifier (i.e., with the same kernel and the same parameters) for both measures and countries across different thresholds. In order to determine the threshold that provides maximum classification accuracy, the latter was calculated while incrementing the percentile threshold to find the maximum accuracy (Fig. 5a,b). This classifier showed that for both countries, the wSDM measure is more accurate than the R measure under all the percentile thresholds, with maximum accuracies emerging between the 25th and the 30th percentile. At the optimum threshold (30th), wSDM achieved an accuracy rate of 70% for Country-1 and of 88.6% for Country-2, while R achieved an accuracy rate of 62.5% for Country-1 and of 84.1% for Country-2. To further analyze the classification scores, we plotted the ROC curves for both countries and both measures under their optimum threshold for each measure (Fig. 5c,d). We can see that higher AUC values were

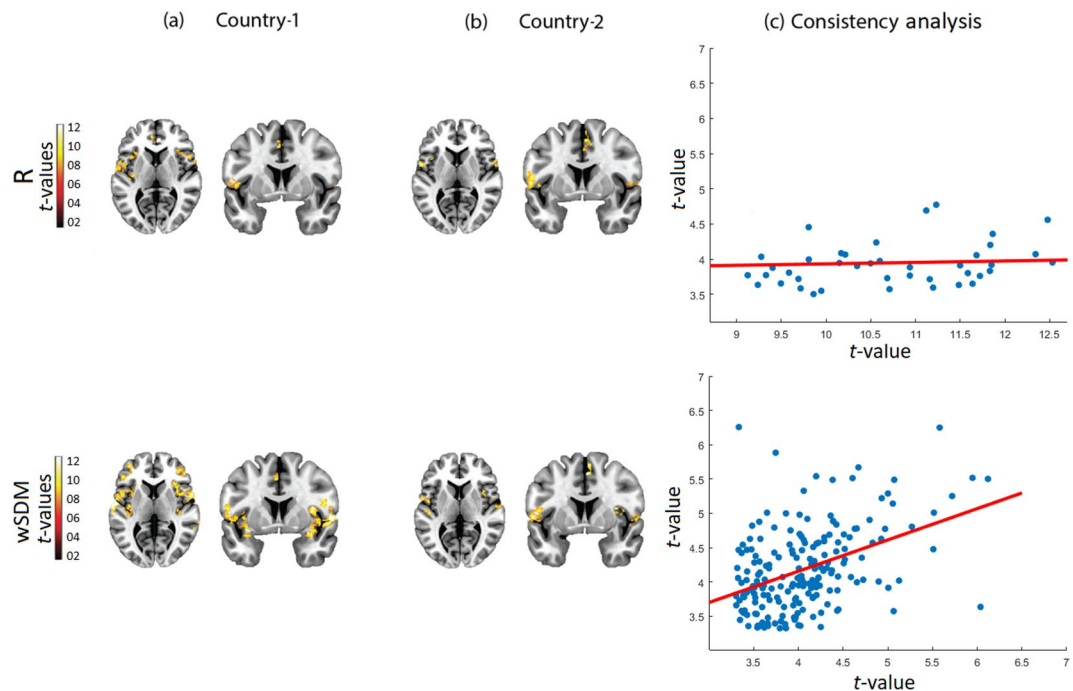


Figure 3. SN bvFTD vs. healthy controls. **(a,b)** Seed connectivity maps (axial plane $z = 3$, coronal plane $y = 6$) comparing HC > bvFTD through a two-sample t -test in the two centers showed a very consistent engagement of the insular cortex and the ACC, two main hubs of the SN. The connectivity volumes have been previously thresholded at the 30th percentile threshold, while the SPM threshold was set to $p = 0.001$, extent threshold = 30 voxels. **(c)** Consistency analysis based on a voxel-wise correlation analysis between the maps (T-values) of both countries. The scale of the axis is not the same between methods given the differences in T-values (data dispersion from the R method would not be well illustrated if identical scales were used for each metric). All brain images are presented according to neurological convention.

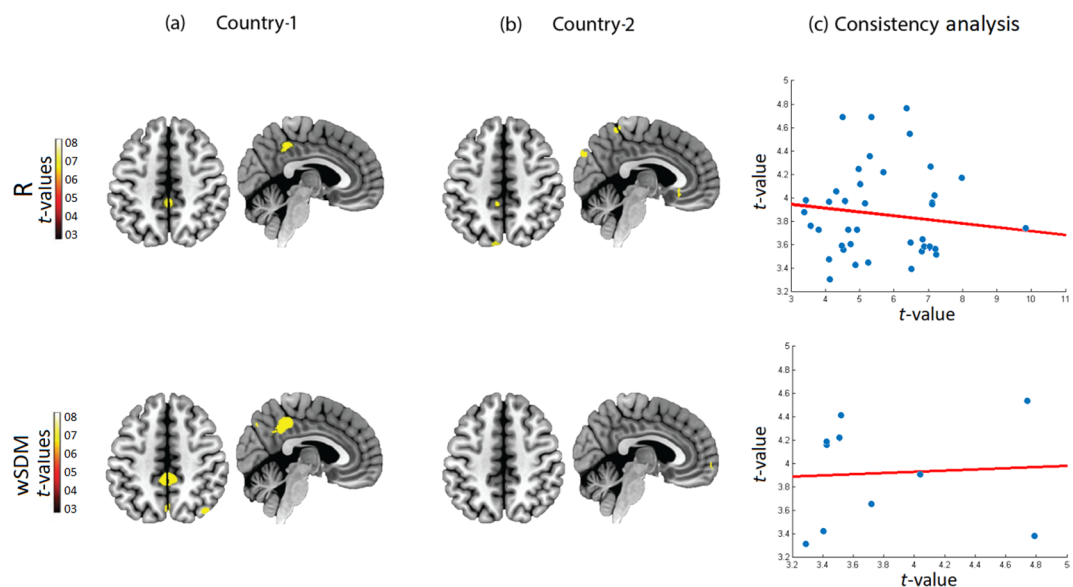


Figure 4. DMN bvFTD vs. healthy controls. **(a,b)** Seed connectivity maps (axial plane $z = 48$, sagittal plane 6) comparing (bvFTD < HC) through a two-sample t -test in the two centers showed a very consistent engagement of the insular cortex and the ACC, two main hubs of the SN. The connectivity volumes have been previously thresholded at the 30th percentile threshold, while the SPM threshold was set to $p = 0.001$, extent threshold = 30 voxels. **(c)** Consistency analysis based on a voxel-wise correlation analysis between the maps (T-values) of both countries. The scale of the axis is not the same between methods given the differences in T-values (data dispersion from the R method would not be well illustrated if identical scales were used for each metric). All brain images are presented according to neurological convention.

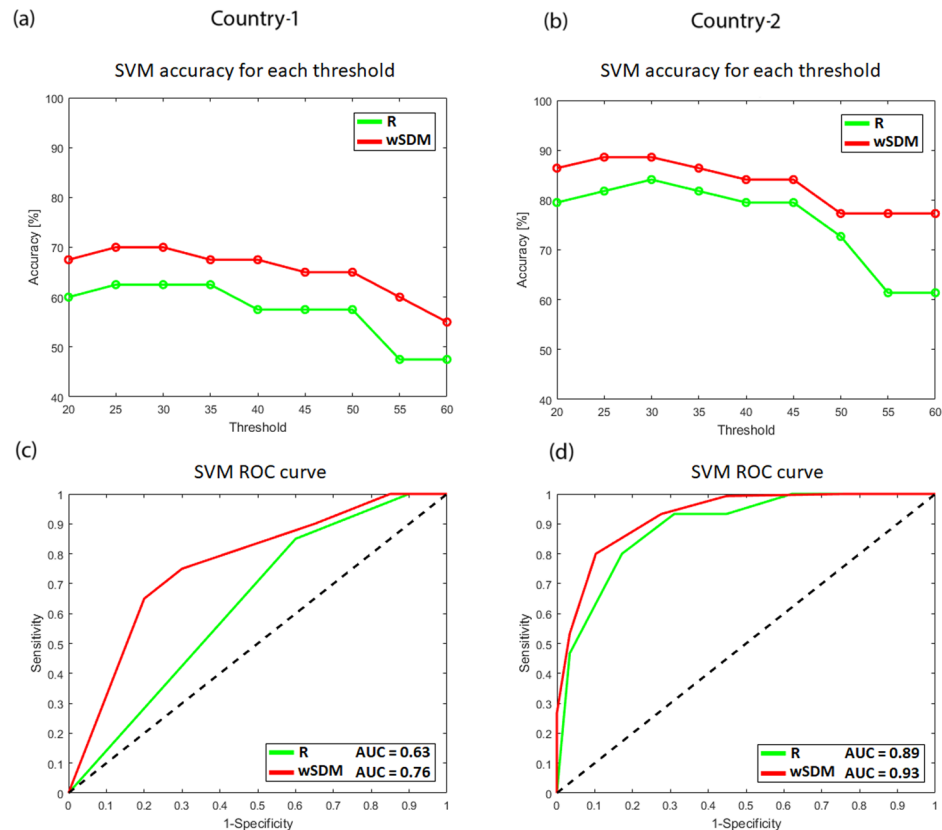


Figure 5. Accuracy and ROC curves for the SVM classifier. **(a,b)** Classification accuracy for Country-1 and Country-2 while varying the percentile threshold, for R and wSDM (see Supplementary Table 3 for details). **(c,d)** ROC curves (AUC significance, $p < 0.01$) [Sensitivity (TPR) vs. 1-Specificity (FPR)] graph for Country-1 and Country-2, for wSDM and R, considering the optimal threshold. The area under the curve (AUC) measures the performance of the classifier across different points of the ROC space. The dashed black line represents random guess (i.e., AUC = 50).

obtained for wSDM relative to R, for both countries (wSDM achieved an AUC of 0.76 for Country-1 and of 0.93 for Country-2, while R achieved an AUC of 0.63 for Country-1 and of 0.89 for Country-2).

The SVM classifier, showed statistically significant differences indicating higher classification rates for wSDM than for R across centers (Country-1: score = 78, $p < 0.001$; and Country-2: score = 63.5, $p = 0.04$). In addition, we also compared the performance of an unweighted symbolic dependence measure (DM) relative to R and wSDM in the two countries, to evaluate the effects of adding the symbolic weights. We found that, although DM yielded better results than R, wSDM outperformed both measures (mean classification rates: for R, 57.22% for Country-1, 75.74% for Country-2; for DM, 63.88% for Country-1, 82.32% for Country-2; and for wSDM, 65.83% for Country-1, 83.58% for Country-2) (see Supplementary Fig. 10 and Supplementary Fig. 11).

We repeated the same analysis using the kNN classifier to test both measures with a non-linear class boundary. We employed this classifier under the same settings and parameters to test for classification accuracy for R and wSDM. As with SVM, we searched the optimal threshold (Fig. 6a,b). For both countries, the wSDM measure was more accurate than R nearly in all percentile thresholds, yielding maximum accuracies between the 25th and the 35th percentile. At its optimal threshold, wSDM achieved an accuracy rate of 80% for Country-1 and of 70.5% for Country-2, while R achieved an accuracy rate of 75% for Country-1 and of 61.4% for Country-2. To further analyze classification scores, we also plotted the ROC curves for both countries and both measures under their optimal threshold for each measure (Fig. 6c,d): higher AUC were obtained for wSDM when compared to R, for both countries (wSDM achieved an AUC of 0.84 for Country-1 and of 0.75 for Country-2, while R achieved an AUC of 0.69 for Country-1 and of 0.67 for Country-2).

In the kNN classifier, we also found significant differences between methods indicating higher classification rates for wSDM compared to R across centers (Country-1: score = 73, $p < 0.001$; and Country-2: score = 60.5, $p = 0.007$). In addition, we repeated the comparison between these measures and DM but with kNN classification values, and we found that wSDM still outperformed both DM and R across countries (mean classification rates: for R, 73.61% for Country-1, 60.37% for Country-2; for DM, 76.11% for Country-1, 58.58% for Country-2; and for wSDM, 77.22% for Country-1, 64.91% for Country-2) (see Supplementary Fig. 12 and Supplementary Fig. 13). Moreover, as a recent study highlighted that partial correlations tend to outperform R in the discrimination between AD patients and healthy controls⁷⁷, we tested the wSDM against this coupling measure. Given that estimating partial correlation for voxel-wise analysis is extremely demanding in computational terms⁷⁸, we

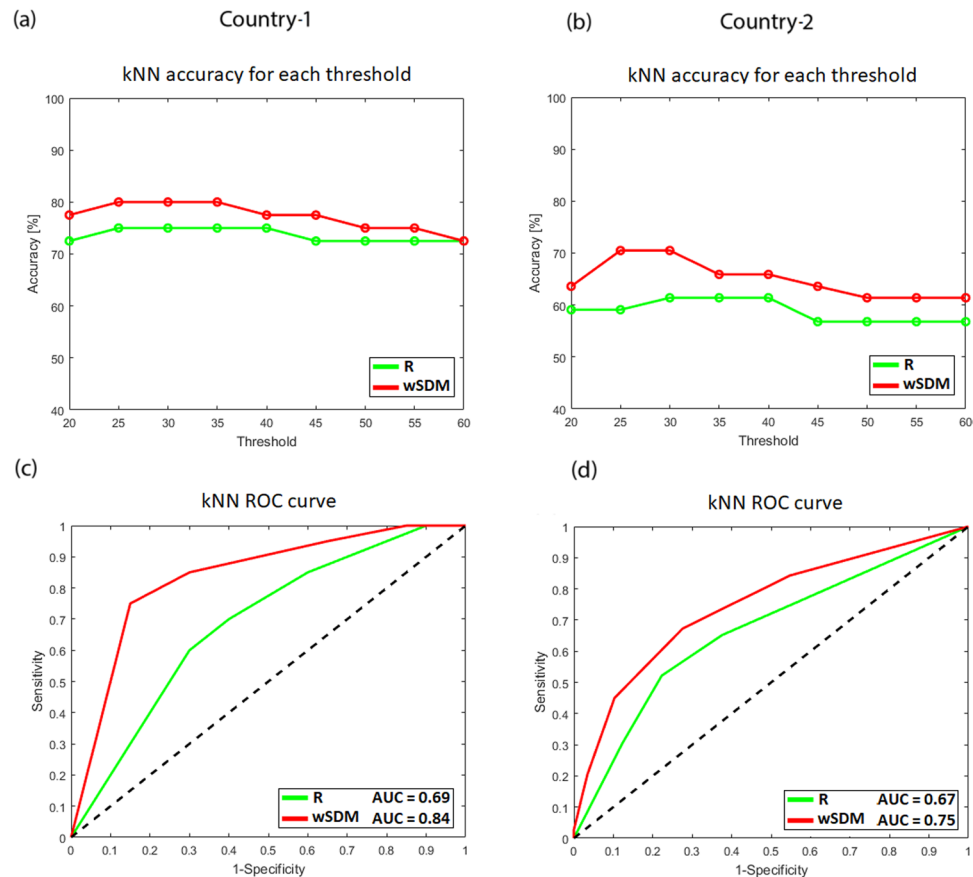


Figure 6. Accuracy and ROC curves for the KNN classifier. **(a,b)** Classification accuracy for Country-1 and Country-2 while varying the percentile threshold (i.e., number of features), for R and wSDM (see Supplementary Table 4 for details). **(c,d)** ROC curves (AUC significance, $p < 0.01$) [Sensitivity (TPR) vs. 1-Specificity (FPR)] graph for Country-1 and Country-2, for wSDM and R, considering the optimal threshold. The area under the curve (AUC) measures the performance of the classifier across different points of the ROC space. The dashed black line represents random guess (i.e., AUC = 50).

followed Vos and colleagues⁷⁷ procedures, and performed the analysis parcellating the brain into large homogeneous regions. To this end, we relied on the Automated Anatomical Labeling (AAL) atlas⁷⁹ –one of the most broadly used atlases in network studies of neurodegenerative diseases^{34,43,80–89} to select the regions related to the SN –as in a previous work of our group⁵¹. Partial correlations and wSDM within the regions of the SN were tested with the same classification methods applied for our seed-based analysis. As expected, in both countries, we found that partial correlations surpassed R but not wSDM classification rates (see Supplementary information 10). Moreover, the wSDM results with this approach were lower than the ones obtained with the seed-based analysis reported in the main manuscript (65% to 67% in the latter, compared to 70% to 88% in the seed-based analysis). This finding further supports the relevance of fine-grained FC data to discriminate patients from healthy controls.

Finally, to test the specificity of the SN for bvFTD, we repeated the same analysis using the DMN and the visual network. In the former, SVM and kNN yielded low mean classification rates (near chance) [SVM for R (50.55% Country-1, 58.61% Country-2) and for wSDM (63.88% Country-1, 69.46% Country-2), and kNN for R (51.38% Country-1, 48.62% Country-2) and for wSDM (52.22% Country-1, 44.71% Country-2)] (Supplementary Tables 6 and 7). Low classification results were also found for the visual network with both methods and in both countries (Supplementary Table 8). In sum, these results highlight the specificity of the SN alterations detected in bvFTD patients.

Discussion

This multicenter study aimed to assess the robustness of the wSDM approach as a novel non-linear association method for fMRI resting-state analysis of neurodegenerative brain networks. Relative to a widely used linear metric (namely, R), the wSDM measure proved superior at identifying resting-state networks, revealing specific differences between bvFTD patients and controls, and classifying groups via machine learning analysis. Notably, such results were consistent despite the heterogeneous acquisition and sociocultural contexts of the centers involved. These findings highlight the potential of wSDM to assess FC based on fMRI data, and, more particularly, to identify sensitive biomarkers in bvFTD (and potentially other neurodegenerative diseases).

Linear vs. non-linear methods. Our novel wSDM measure outperformed R in the detection and analysis of resting-state networks. First, based on a seed analysis, the wSDM successfully identified two well-characterized resting-state networks in healthy subjects, namely: the DMN and the SN^{38,44,52,90}. While this was also possible with R, the wSDM approach evinced higher consistency across centers with heterogeneous acquisition conditions. This result suggests that a measure which captures both linear and non-linear connectivity, such as wSDM, could prove more reliable and resistant against the variability of data with diverse characteristics and from different sources. The same was true in the comparison between patients and controls. Relative to R, wSDM revealed more consistent alterations of the SN (a hallmark disturbance in bvFTD^{5,6,43}) across countries. Yet, both methods presented inconsistent results across centers when the DMN was analyzed. This pattern of results was expected given that previous studies have reported null or reduced hypo-connectivity differences within this network in bvFTD^{42,72–74}. Moreover, the visual network also failed to show consistent differences between samples. Taken together, our findings reinforce the specificity of SN disturbances as a potential hallmark of bvFTD. Additional support for the robustness of wSDM came from the machine learning analysis. Two different approaches (based on linear or non-linear boundaries) showed that this measure achieved significantly higher classification rates than R in both countries. As before, this result was based on the FC of the SN, while the DMN and the visual network presented classification rates near chance. Such findings further evince the relevance of a measure that combines both linear and non-linear properties for obtaining consistent results in heterogeneous contexts.

Although brain function presents non-linear properties^{15,17,91,92}, the implementation of non-linear FC methods has yielded inconsistent results as compared to linear ones. Non-linear measures have been found to provide useful information to discriminate patients (e.g., in consciousness impairments and schizophrenia) and different experimental conditions^{93–95}. For example, an EEG study found that MI measures superseded Pearson, Spearman, and Kendall correlations in discriminating between brain states⁹³. In addition, MI also outperformed the traditional general lineal model in establishing significant differences between specific stimulus types via fMRI correlates⁹⁴. However, while non-linear brain connectivity analysis on schizophrenia using a measure based on MI found disease-specific pathological non-linear connections, this approach did not prove superior to R in classifying between patients and healthy controls⁹⁵. Moreover, another fMRI study on schizophrenia found higher differences in FC between patients and controls via linear correlation than through MI²³. In addition, other non-linear approaches to EEG research, such as wSMI, have been observed to surpass traditional FC measures like Phase Locking Value and Phase Lag Index in detecting patients with consciousness impairments¹⁸. However, these robust features are not inherent to *any* non-linear method, especially when considering fMRI data. Indeed, a resting-state fMRI study showed that, while non-gaussianity was present in the FC signal, the portion of information neglected by linear correlation amounted to only 5% compared to MI¹³. These findings cast doubts on the practical relevance of standard non-linear methods in fMRI. However, the specific non-linear measures applied so far in the field are undermined by the intrinsic low time-resolution of the technique, which hinders a reliable estimation of MI by using a standard histogram approach. In addition, those measures do not capture the temporal dimension of the signal, providing a static representation of FC which may ignore relevant time features of the BOLD signal.

Compared to FC analyses in the above fMRI studies, the wSDM presents two methodological advantages that might explain our positive results. First, its symbolic approach allows to partially capturing the temporal history information of the BOLD signal for estimating associations between regions. While most connectivity measures (linear or non-linear) are blind to this temporal dimension of the signal³⁶, the wSDM measure contemplates the time order of neighboring data-points to produce symbols, and allows characterizing FC both locally (within symbols) and globally (across strings) based on the temporal history pattern of the BOLD signal. Moreover, by using weights based on symbolic similarity, associations that are incoherent in time are yield near-zero values, thus reducing FC false positives and augmenting the robustness of detected patterns. Previous studies have shown the relevance of considering the temporal dimension of FC^{12,14,36}. For example, it has been essential for discriminating between patients with consciousness impairments via EEG signals¹⁸. Moreover, in fMRI, it improves diagnostic power in Alzheimer's disease⁹⁶ and allows for the detection of transient dysconnectivity of resting-state networks in schizophrenia patients⁹⁷. Second, to overcome the limitation of the low temporal resolution of fMRI data, we applied a copula-based dependence measure, namely the Hoeffding Phi-Square⁶⁰, which is based on copula functions that link the probability of joint and marginal signal distributions to measure dependence. Instead of approximating the distributions via a histogram to calculate MI, which may lead to inconsistent results, the copula-based approach is resistant to the effect of outliers because it is based on rank statistics³¹ and, hence, it might be more robust to estimate common features across heterogeneous data, as in the case of our study.

In sum, our report supports the sensitivity of the wSDM measure and shows that weighted MI metrics could be particularly sensitive to analyze FC from fMRI data. The consistency of our findings despite heterogeneity in acquisition methods and socio-cultural features of the data samples highlights the potential of wSDM as a robust metric for establishing widely applicable biomarkers.

Relevance for neurodegeneration studies. Like other neurodegenerative conditions, FTD impacts household economies and health systems worldwide^{98–101}. Finding robust and effective biomarkers for its early detection is thus crucial for the implementation of new re-habilitation and intervention methods to alleviate the impact of these conditions^{102,103}. FC has been proposed as a potential biomarker of neurodegenerative diseases^{4,5,104}, with recent studies on bvFTD focusing on SN connectivity^{41,42}. However, so far linear measures have yielded inconsistent results, concluding that this network could be either altered or preserved in symptomatic and pre-symptomatic stages^{41,42}. Moreover, the specificity of SN alterations also proves controversial, given that other resting-state networks (e.g., the DMN) can be affected in bvFTD^{73,105}, whereas the SN can also be altered in other diseases^{106,107}. In addition, a previous study based on linear correlation measures, showed that SN differences between controls and patients were not consistent across different recordings' centers¹⁰.

Importantly, all these studies were based on linear correlation indexes. Thus, in light of our present findings, we propose that a dependence measure such as wSDM could potentially circumvent the inconsistency of extant FC results. Relatively few studies have employed non-linear connectivity methods to tap into pathology-specific FC alterations in neurodegeneration. Synchronization likelihood (SL)¹⁰⁸, has been used to show abnormalities on long-range networks in AD patients with EEG¹⁰⁹ and MEG¹¹⁰. As mentioned before, in dementia research, the wSMI approach was applied only in one previous EEG studies, in which it proved to be a robust biomarker for bvFTD²⁹. This dependency measure has never been used to analyze FC in dementia patients given the methodological constraints of the fMRI signal (low time/frequency resolution) for its application. Here, we circumvent this issue by employing a copula-based approach to estimate FC based on wSDM. In addition, we showed that this measure was, compared to a linear method (R), more consistent across centers in the identification of resting-state networks, and in the discrimination and classification of patients from healthy participants.

In this way, our findings proved to be robust against acquisition heterogeneity. On the one hand, the use of statistical copulas based on non-parametric rank statistics are more resilient to outliers than parametric measures such as R, hence providing consistent results even over MR acquisitions with different signal-to-noise ratio. On the other, the symbolic weights capture transient brain activity that conventional methods, such as R and MI, may disregard as noise. Moreover, a static FC measure provides an averaged connectivity pattern across acquisition time, which may undermine FC sensitivity. By capturing these key properties of FC despite the heterogeneity of the samples and fMRI parameters, wSDM may afford sensitive biomarkers for neurodegenerative diseases across clinical centers^{111,112}.

In sum, we found that the wSDM measure outperformed linear measures across centers in the discrimination and classification of patients based on the SN, and that these results were specific for this network (given an absence of consistent differences in the DMN and the visual network). Considering the underemployment of nonlinear measures to study neurodegenerative diseases in fMRI, and the variability of the results reported in previous research, our findings highlights the potential value of wSDM as a novel biomarker measure for neurodegenerative disease, although further research is needed.

Limitations and future studies. A major limitation of this study is the moderate sample size from each center. However, similar works have reported valid, replicable results with similar or smaller samples^{44,73}, and our findings prove consistent across centers and relative to previous studies^{5,43}. Nevertheless, future research should test the robustness of this measure compared to linear approaches in at least two critical scenarios. First, replication studies should be conducted with larger samples, to establish whether reduced variability related to increased data availability reduces the differences between linear and non-linear methods. Second, multiple single-case analyses would be highly informative to establish the potential of our metric for diagnostic and follow-up purpose in clinical settings¹¹³.

Although several different regions and coordinates can be selected for seed-based analysis, we have used areas that are targets of each of the evaluated networks, namely, the SN⁹⁰, the DMN⁵², and the visual network⁵³. Moreover, we showed that the wSDM outperformed R in the characterization of all of them, which highlights the potential generalization of our non-linear method to network research beyond the selection of specific areas and coordinates for a given seed.

Looking forward, the sensitivity and specificity of wSDM should be tested in future studies including a contrastive pathological group. Also, future research in this line should also include clinical data to analyze potential associations between FC and the patients' cognitive decline, as done elsewhere in the literature^{27,29,51}.

Conclusion

Resting state FC from fMRI data represents a promising tool for the development of early biomarkers for neurodegenerative disorders. However, despite that brain connectivity presents both linear and non-linear components, most dementia research in fMRI is based on linear dependency measures. This oversimplifying approach might explain the controversy results regarding the sensitivity and specificity of FC on these diseases. Here, we found that a novel non-linear connectivity measure consistently outperformed a linear one in the discrimination and classification of bvFTD patients from healthy participants across different centers. Our findings suggest that the wSDM might be robust against acquisition parameter heterogeneity and, hence, it has a potential value as a biomarker for neurodegenerative diseases.

References

1. Fox, M. *et al.* The human brain is intrinsically organized into dynamic, anticorrelated functional networks. *Proc Natl Acad Sci USA* **102**, 9673–9678 (2005).
2. Fox, M. D. & Raichle, M. Spontaneous fluctuations in brain activity observed with functional magnetic resonance imaging. *Nat Rev Neurosci* **8**, 700–711 (2007).
3. Rubinov, M. & Sporns, O. Complex network measures of brain connectivity: uses and interpretations. *NeuroImage* **52**, 1059–1069, <https://doi.org/10.1016/j.neuroimage.2009.10.003> (2010).
4. Buckner, R. L. *et al.* Cortical hubs revealed by intrinsic functional connectivity: mapping, assessment of stability, and relation to Alzheimer's disease. *The Journal of neuroscience: the official journal of the Society for Neuroscience* **29**, 1860–1873, <https://doi.org/10.1523/JNEUROSCI.5062-08.2009> (2009).
5. Pievani, M., de Haan, W., Wu, T., Seeley, W. W. & Frisoni, G. B. Functional network disruption in the degenerative dementias. *The Lancet. Neurology* **10**, 829–843, [https://doi.org/10.1016/S1474-4422\(11\)70158-2](https://doi.org/10.1016/S1474-4422(11)70158-2) (2011).
6. Pievani, M., Filippini, N., van den Heuvel, M. P., Cappa, S. F. & Frisoni, G. B. Brain connectivity in neurodegenerative diseases—from phenotype to proteinopathy. *Nature reviews. Neurology* **10**, 620–633, <https://doi.org/10.1038/nrneurol.2014.178> (2014).
7. Greicius, M. D. *et al.* Resting-state functional connectivity in neuropsychiatric disorders. *Curr Opin Neurol* **21**, 424–430 (2008).

8. Palop, J. J., Chin, J. & Mucke, L. A network dysfunction perspective on neurodegenerative diseases. *Nature* **443**, 768–773, <https://doi.org/10.1038/nature05289> (2006).
9. Seeley, W. W., Crawford, R. K., Zhou, J., Miller, B. L. & Greicius, M. D. Neurodegenerative diseases target large-scale human brain networks. *Neuron* **62**, 42–52, <https://doi.org/10.1016/j.neuron.2009.03.024> (2009).
10. Sedeño, L. *et al.* Tackling variability: A multicenter study to provide a gold-standard network approach for frontotemporal dementia. *Hum Brain Mapp.* (2017).
11. Biswal, B. B. *et al.* Toward discovery science of human brain function. *Proceedings of the National Academy of Sciences of the United States of America* **107**, 4734–4739, <https://doi.org/10.1073/pnas.0911855107> (2010).
12. Cabral, J., Kringelbach, M. L. & Deco, G. Exploring the network dynamics underlying brain activity during rest. *Progress in neurobiology* **114**, 102–131, <https://doi.org/10.1016/j.pneurobio.2013.12.005> (2014).
13. Hlinka, J., Palus, M., Vejmelka, M., Mantini, D. & Corbetta, M. Functional connectivity in resting-state fMRI: is linear correlation sufficient? *NeuroImage* **54**, 2218–2225, <https://doi.org/10.1016/j.neuroimage.2010.08.042> (2011).
14. Breakspear, M. Dynamic models of large-scale brain activity. *Nature neuroscience* **20**, 340–352, <https://doi.org/10.1038/nn.4497> (2017).
15. Gultepe, E. & He, B. A linear/nonlinear characterization of resting state brain networks in FMRI time series. *Brain topography* **26**, 39–49, <https://doi.org/10.1007/s10548-012-0249-7> (2013).
16. Stam, C. J. Nonlinear dynamical analysis of EEG and MEG: review of an emerging field. *Clin Neurophysiol* **116**, 2266–2301, <https://doi.org/10.1016/j.clinph.2005.06.011> (2005).
17. Lahaye, P., Poline, J. B., Flandin, G., Dodel, S. & Garnero, L. Functional connectivity: studying nonlinear, delayed interactions between BOLD signals. *NeuroImage* **20**, 962–974, [https://doi.org/10.1016/s1053-8119\(03\)00340-9](https://doi.org/10.1016/s1053-8119(03)00340-9) (2003).
18. King, J. R. *et al.* Information sharing in the brain indexes consciousness in noncommunicative patients. *Current biology: CB* **23**, 1914–1919, <https://doi.org/10.1016/j.cub.2013.07.075> (2013).
19. de Zwart, J. A. *et al.* Hemodynamic nonlinearities affect BOLD fMRI response timing and amplitude. *NeuroImage* **47**, 1649–1658, <https://doi.org/10.1016/j.neuroimage.2009.06.001> (2009).
20. Xie, X., Cao, Z. & Weng, X. Spatiotemporal nonlinearity in resting-state fMRI of the human brain. *NeuroImage* **40**, 1672–1685, <https://doi.org/10.1016/j.neuroimage.2008.01.007> (2008).
21. Stam, C. J. Nonlinear dynamical analysis of EEG and MEG: review of an emerging field. *Clinical neurophysiology: official journal of the International Federation of Clinical Neurophysiology* **116**, 2266–2301, <https://doi.org/10.1016/j.clinph.2005.06.011> (2005).
22. Wang, H. E. *et al.* A systematic framework for functional connectivity measures. *Frontiers in neuroscience* **8**, 405, <https://doi.org/10.3389/fnins.2014.00405> (2014).
23. Ince, R. A. *et al.* A statistical framework for neuroimaging data analysis based on mutual information estimated via a gaussian copula. *Human brain mapping* **38**, 1541–1573, <https://doi.org/10.1002/hbm.23471> (2017).
24. Lynall, M. E. *et al.* Functional connectivity and brain networks in schizophrenia. *The Journal of neuroscience: the official journal of the Society for Neuroscience* **30**, 9477–9487, <https://doi.org/10.1523/JNEUROSCI.0333-10.2010> (2010).
25. Bandt, C. & Pompe, B. Permutation entropy: a natural complexity measure for time series. *Physical review letters* **88**, 174102, <https://doi.org/10.1103/PhysRevLett.88.174102> (2002).
26. Hesse, E. *et al.* Early detection of intentional harm in the human amygdala. *Brain: a journal of neurology* **139**, 54–61, <https://doi.org/10.1093/brain/awv336> (2016).
27. Garcia-Cordero, I. *et al.* Attention, in and Out: Scalp-Level and Intracranial EEG Correlates of Interoception and Exteroception. *Frontiers in neuroscience* **11**, 411, <https://doi.org/10.3389/fnins.2017.00411> (2017).
28. Melloni, M. *et al.* Cortical dynamics and subcortical signatures of motor-language coupling in Parkinson's disease. *Scientific reports* **5**, 11899, <https://doi.org/10.1038/srep11899> (2015).
29. Dottori, M. *et al.* Towards affordable biomarkers of frontotemporal dementia: A classification study via network's information sharing. *Sci Rep.* **7**, 3822 (2017).
30. Nelsen, R. *An Introduction to Copulas* (Springer Series in Statistics) (2006).
31. Poczos, B., Krishner, S., Pal, D., Szepesvari, C. & Schneider, J. Robust Nonparametric Copula Based Dependence Estimators. *Proceedings of NIPS 2011 Workshop on Copulas in Machine Learning* (2011).
32. Schweizer, B. & Wolff, E. F. On Nonparametric Measures of Dependence for Random Variables. *The Annals of Statistics* **9**, 879–885 (1981).
33. Hoeffding, W. Masstabinvariante Korrelationstheorie. *Schrift. Math. Seminars Inst. Angew. Math. Univ. Berlin* **5**, 181–233 (1940).
34. Ding, A. & Li, Y. Copula correlation: An equitable dependence measure and extension of pearson's correlation. *arXiv preprint arXiv 1312.7214* (2013).
35. Karahanoglu, F. I. & V D Ville, D. Transient brain activity disentangles fMRI resting-state dynamics in terms of spatially and temporally overlapping networks. *Nat Commun.* (2015).
36. Hutchison, R. M. *et al.* Dynamic functional connectivity: promise, issues, and interpretations. *NeuroImage* **80**, 360–378, <https://doi.org/10.1016/j.neuroimage.2013.05.079> (2013).
37. Leonardi, N. *et al.* Principal components of functional connectivity: a new approach to study dynamic brain connectivity during rest. *NeuroImage* **83**, 937–950, <https://doi.org/10.1016/j.neuroimage.2013.07.019> (2013).
38. Piguet, O., Hornberger, M., Mioshi, E. & Hodges, J. R. Behavioural-variant frontotemporal dementia: diagnosis, clinical staging, and management. *The Lancet. Neurology* **10**, 162–172, [https://doi.org/10.1016/S1474-4422\(10\)70299-4](https://doi.org/10.1016/S1474-4422(10)70299-4) (2011).
39. Ibañez, A. & Manes, F. Contextual social cognition and the behavioral variant of frontotemporal dementia. *Neurology* **78**, 1354–1362 (2012).
40. Menon, V. & Uddin, L. Q. Saliency, switching, attention and control: a network model of insula function. *Brain structure & function* **214**, 655–667, <https://doi.org/10.1007/s00429-010-0262-0> (2010).
41. Dopper, E. G. *et al.* Structural and functional brain connectivity in presymptomatic familial frontotemporal dementia. *Neurology* **83**, 19–26 (2014).
42. Whitwell, J. L. *et al.* Altered functional connectivity in asymptomatic MAPT subjects: a comparison to bvFTD. *Neurology* **77**, 866–874 (2011).
43. Agosta, F. *et al.* Brain network connectivity assessed using graph theory in frontotemporal dementia. *Neurology* **81**, 134–143, <https://doi.org/10.1212/WNL.0b013e31829a33f8> (2013).
44. Greicius, M. D., Srivastava, G., Reiss, A. L. & Menon, V. Default-mode network activity distinguishes Alzheimer's disease from healthy aging: evidence from functional MRI. *Proceedings of the National Academy of Sciences of the United States of America* **101**, 4637–4642, <https://doi.org/10.1073/pnas.0308627101> (2004).
45. Rascovsky, K. *et al.* Sensitivity of revised diagnostic criteria for the behavioural variant of frontotemporal dementia. *Brain: a journal of neurology* **134**, 2456–2477, <https://doi.org/10.1093/brain/awr179> (2011).
46. Baez, S. *et al.* Comparing moral judgments of patients with frontotemporal dementia and frontal stroke. *JAMA neurology* **71**, 1172–1176, <https://doi.org/10.1001/jamaneuro.2014.347> (2014).
47. Torralva, T., Roca, M., Gleichgerrcht, E., Bekinschtein, T. & Manes, F. A neuropsychological battery to detect specific executive and social cognitive impairments in early frontotemporal dementia. *Brain: a journal of neurology* **132**, 1299–1309, <https://doi.org/10.1093/brain/awp041> (2009).

48. Nichols, T. E. *et al.* Best practices in data analysis and sharing in neuroimaging using MRI. *Nature neuroscience* **20**, 299–303, <https://doi.org/10.1038/nn.4500> (2017).
49. Poldrack, R. A. *et al.* Scanning the horizon: towards transparent and reproducible neuroimaging research. *Nat Rev Neurosci* **18**, 115–126, <https://doi.org/10.1038/nrn.2016.167> (2017).
50. Chao-Gan, Y. & Yu-Feng, Z. DPARSF: A MATLAB Toolbox for “Pipeline” Data Analysis of Resting-State fMRI. *Frontiers in systems neuroscience* **4**, 13, <https://doi.org/10.3389/fnsys.2010.00013> (2010).
51. Seden, L. *et al.* Brain Network Organization and Social Executive Performance in Frontotemporal Dementia. *Journal of the International Neuropsychological Society: JINS* **22**, 250–262, <https://doi.org/10.1017/S1355617715000703> (2016).
52. Uddin, L. Q., Kelly, A. M., Biswal, B. B., Castellanos, F. X. & Milham, M. P. Functional connectivity of default mode network components: correlation, anticorrelation, and causality. *Human brain mapping* **30**, 625–637, <https://doi.org/10.1002/hbm.20531> (2009).
53. Shirer, W. R., Ryali, S., Rykhlevskaia, E., Menon, V. & Greicius, M. D. Decoding subject-driven cognitive states with whole-brain connectivity patterns. *Cerebral cortex* **22**, 158–165, <https://doi.org/10.1093/cercor/bhr099> (2012).
54. Melloni, M. *et al.* Your perspective and my benefit: multiple lesion models of self-other integration strategies during social bargaining. *Brain: a journal of neurology* **139**, 3022–3040, <https://doi.org/10.1093/brain/aww231> (2016).
55. van den Heuvel, M. P. *et al.* Proportional thresholding in resting-state fMRI functional connectivity networks and consequences for patient-control connectome studies: Issues and recommendations. *NeuroImage* **152**, 437–449, <https://doi.org/10.1016/j.neuroimage.2017.02.005> (2017).
56. Kinney, J. & Atwal, G. Equitability, mutual information, and the maximal information coefficient. *Proc Natl Acad Sci USA* **111**, 3354–3359 (2014).
57. Cover, T. & Thomas, J. Elements of Information Theory. John Wiley and Sons (1991).
58. Kirshner, S. & Póczos, B. ICA and ISA Using Schweizer-Wolff Measure of Dependence. *Proceedings of the 25th international conference on Machine learning*, 464–471 (2008).
59. Sklar, A. Fonctions de repartition ‘a’ n dimensions et leurs marges. *Publ. Inst. Statist. Univ. Paris* **8** (1959).
60. Gaißer, S., Ruppert, M. & Schmid, F. A multivariate version of Hoeffding’s Phi-Square. *Journal of Multivariate Analysis* **101**, 2571–2586, <https://doi.org/10.1016/j.jmva.2010.07.006> (2010).
61. Szabo, Z. Information Theoretical Estimators Toolbox. *Journal of Machine Learning Research* **15** (2014).
62. von der Malsburg, C., Phillips, W. & Singer, W. Dynamic Coordination in the Brain: From Neurons to Mind. The MIT Press. (2010).
63. Rabinovich, M., Friston, K. & Varona, P. Principles of Brain Dynamics: Global State Interactions. The MIT Press. (2012).
64. Lesk, A. Introduction to Bioinformatics. Oxford University Press (2002).
65. Cawley, G. C. & Talbot, N. L. C. On over-fitting in model selection and subsequent selection bias in performance evaluation. *J Mach Learn Res* **11**, 2079–2107 (2010).
66. Beckmann, C. F., DeLuca, M., Devlin, J. T. & Smith, S. M. Investigations into resting-state connectivity using independent component analysis. *Philosophical transactions of the Royal Society of London. Series B, Biological sciences* **360**, 1001–1013, <https://doi.org/10.1098/rstb.2005.1634> (2005).
67. Damoiseaux, J. S. *et al.* Consistent resting-state networks across healthy subjects. *Proceedings of the National Academy of Sciences of the United States of America* **103**, 13848–13853, <https://doi.org/10.1073/pnas.0601417103> (2006).
68. Smith, S. M. *et al.* Correspondence of the brain’s functional architecture during activation and rest. *Proceedings of the National Academy of Sciences of the United States of America* **106**, 13040–13045, <https://doi.org/10.1073/pnas.0905267106> (2009).
69. van den Heuvel, M. P., Stam, C. J., Boersma, M. & Hulshoff Pol, H. E. Small-world and scale-free organization of voxel-based resting-state functional connectivity in the human brain. *NeuroImage* **43**, 528–539, <https://doi.org/10.1016/j.neuroimage.2008.08.010> (2008).
70. Woo, C. W., Krishnan, A. & Wager, T. D. Cluster-extent based thresholding in fMRI analyses: pitfalls and recommendations. *NeuroImage* **91**, 412–419, <https://doi.org/10.1016/j.neuroimage.2013.12.058> (2014).
71. Poldrack, R. A. *et al.* Guidelines for reporting an fMRI study. *NeuroImage* **40**, 409–414, <https://doi.org/10.1016/j.neuroimage.2007.11.048> (2008).
72. Farb, N. A. *et al.* Abnormal network connectivity in frontotemporal dementia: evidence for prefrontal isolation. *Cortex; a journal devoted to the study of the nervous system and behavior* **49**, 1856–1873, <https://doi.org/10.1016/j.cortex.2012.09.008> (2013).
73. Zhou, J. *et al.* Divergent network connectivity changes in behavioural variant frontotemporal dementia and Alzheimer’s disease. *Brain: a journal of neurology* **133**, 1352–1367, <https://doi.org/10.1093/brain/awq075> (2010).
74. Filippi, M. *et al.* Functional network connectivity in the behavioral variant of frontotemporal dementia. *Cortex; a journal devoted to the study of the nervous system and behavior* **49**, 2389–2401, <https://doi.org/10.1016/j.cortex.2012.09.017> (2013).
75. Friston, K. J., Ashburner, J. T., Kiebel, S. J., Nichols, T. E. & Penny, W. D. Statistical Parametric Mapping: the Analysis of Functional Brain Images. Elsevier/Academic Press (2007).
76. Pereira, F., Mitchell, T. & Botvinick, M. Machine learning classifiers and fMRI: a tutorial overview. *NeuroImage* **45**, S199–209, <https://doi.org/10.1016/j.neuroimage.2008.11.007> (2009).
77. de Vos, F. *et al.* A comprehensive analysis of resting state fMRI measures to classify individual patients with Alzheimer’s disease. *NeuroImage* **167**, 62–72, <https://doi.org/10.1016/j.neuroimage.2017.11.025> (2018).
78. Wang, Y., Kang, J., Kemmer, P. B. & Guo, Y. An Efficient and Reliable Statistical Method for Estimating Functional Connectivity in Large Scale Brain Networks Using Partial Correlation. *Frontiers in neuroscience* **10**, 123, <https://doi.org/10.3389/fnins.2016.00123> (2016).
79. Tzourio-Mazoyer, N. *et al.* Automated anatomical labeling of activations in SPM using a macroscopic anatomical parcellation of the MNI MRI single-subject brain. *NeuroImage* **15**, 273–289, <https://doi.org/10.1006/nimg.2001.0978> (2002).
80. Baggio, H. C. *et al.* Functional brain networks and cognitive deficits in Parkinson’s disease. *Human brain mapping* **35**, 4620–4634, <https://doi.org/10.1002/hbm.22499> (2014).
81. Liu, Z. *et al.* Altered topological patterns of brain networks in mild cognitive impairment and Alzheimer’s disease: a resting-state fMRI study. *Psychiatry research* **202**, 118–125, <https://doi.org/10.1016/j.psychres.2012.03.002> (2012).
82. Sanabria-Diaz, G., Martinez-Montes, E., Melie-Garcia, L. & Alzheimer’s Disease Neuroimaging, I. Glucose metabolism during resting state reveals abnormal brain networks organization in the Alzheimer’s disease and mild cognitive impairment. *PLoS one* **8**, e68860, <https://doi.org/10.1371/journal.pone.0068860> (2013).
83. Sanz-Arigita, E. J. *et al.* Loss of ‘small-world’ networks in Alzheimer’s disease: graph analysis of FMRI resting-state functional connectivity. *PLoS one* **5**, e13788, <https://doi.org/10.1371/journal.pone.0013788> (2010).
84. Seo, E. H. *et al.* Influence of APOE genotype on whole-brain functional networks in cognitively normal elderly. *PLoS one* **8**, e83205, <https://doi.org/10.1371/journal.pone.0083205> (2013).
85. Seo, E. H. *et al.* Whole-brain functional networks in cognitively normal, mild cognitive impairment, and Alzheimer’s disease. *PLoS one* **8**, e53922, <https://doi.org/10.1371/journal.pone.0053922> (2013).
86. Supekar, K., Menon, V., Rubin, D., Musen, M. & Greicius, M. D. Network analysis of intrinsic functional brain connectivity in Alzheimer’s disease. *PLoS computational biology* **4**, e1000100, <https://doi.org/10.1371/journal.pcbi.1000100> (2008).
87. Tijms, B. M. *et al.* Single-subject gray matter graph properties and their relationship with cognitive impairment in early- and late-onset Alzheimer’s disease. *Brain connectivity* **4**, 337–346, <https://doi.org/10.1089/brain.2013.0209> (2014).

88. Xiang, J., Guo, H., Cao, R., Liang, H. & Chen, J. An abnormal resting-state functional brain network indicates progression towards Alzheimer's disease. *Neural regeneration research* **8**, 2789–2799, <https://doi.org/10.3969/j.issn.1673-5374.2013.30.001> (2013).
89. Yao, Z. *et al.* Abnormal cortical networks in mild cognitive impairment and Alzheimer's disease. *PLoS computational biology* **6**, e1001006, <https://doi.org/10.1371/journal.pcbi.1001006> (2010).
90. Seeley, W. W. *et al.* Dissociable intrinsic connectivity networks for salience processing and executive control. *The Journal of neuroscience: the official journal of the Society for Neuroscience* **27**, 2349–2356, <https://doi.org/10.1523/JNEUROSCI.5587-06.2007> (2007).
91. Hartman, D., Hlinka, J., Palus, M., Mantini, D. & Corbetta, M. The role of nonlinearity in computing graph-theoretical properties of resting-state functional magnetic resonance imaging brain networks. *Chaos* **21**, 013119, <https://doi.org/10.1063/1.3553181> (2011).
92. Le Van Quyen, M., Chavez, M., Rudrauf, D. & Martinerie, J. Exploring the nonlinear dynamics of the brain. *Journal of physiology, Paris* **97**, 629–639, <https://doi.org/10.1016/j.jphysparis.2004.01.019> (2003).
93. Bonita, J. D. *et al.* Time domain measures of inter-channel EEG correlations: a comparison of linear, nonparametric and nonlinear measures. *Cognitive neurodynamics* **8**, 1–15, <https://doi.org/10.1007/s11571-013-9267-8> (2014).
94. Gomez-Verdejo, V., Martinez-Ramon, M., Florensa-Vila, J. & Oliviero, A. Analysis of fMRI time series with mutual information. *Medical image analysis* **16**, 451–458, <https://doi.org/10.1016/j.media.2011.11.002> (2012).
95. Su, L., Wang, L., Shen, H., Feng, G. & Hu, D. Discriminative analysis of non-linear brain connectivity in schizophrenia: an fMRI Study. *Frontiers in human neuroscience* **7**, 702, <https://doi.org/10.3389/fnhum.2013.00702> (2013).
96. Chen, X. *et al.* Extraction of dynamic functional connectivity from brain grey matter and white matter for MCI classification. *Human brain mapping* **38**, 5019–5034, <https://doi.org/10.1002/hbm.23711> (2017).
97. Damaraju, E. *et al.* Dynamic functional connectivity analysis reveals transient states of dysconnectivity in schizophrenia. *NeuroImage. Clinical* **5**, 298–308, <https://doi.org/10.1016/j.nicl.2014.07.003> (2014).
98. Rodriguez, J. J. L. *et al.* Prevalence of dementia in Latin America, India, and China: a population-based cross-sectional survey. *The Lancet* **372**, 464–474, [https://doi.org/10.1016/s0140-6736\(08\)61002-8](https://doi.org/10.1016/s0140-6736(08)61002-8) (2008).
99. Santini, Z. I. *et al.* Social network typologies and mortality risk among older people in China, India, and Latin America: A 10/66 Dementia Research Group population-based cohort study. *Social science & medicine* **147**, 134–143, <https://doi.org/10.1016/j.socscimed.2015.10.061> (2015).
100. Sosa, A. L. *et al.* Population normative data for the 10/66 Dementia Research Group cognitive test battery from Latin America, India and China: a cross-sectional survey. *BMC neurology* **9**, 48, <https://doi.org/10.1186/1471-2377-9-48> (2009).
101. Prince, M., Comas-Herrera, A., Knapp, M., Guerchet, M. & Karagiannidou, M. World Alzheimer report 2016: improving healthcare for people living with dementia: coverage, quality and costs now and in the future. London: UK: Alzheimer's Disease International (ADI) (2016).
102. Wang, J., Redmond, S. J., Bertoux, M., Hodges, J. R. & Hornberger, M. A Comparison of Magnetic Resonance Imaging and Neuropsychological Examination in the Diagnostic Distinction of Alzheimer's Disease and Behavioral Variant Frontotemporal Dementia. *Frontiers in aging neuroscience* **8**, 119, <https://doi.org/10.3389/fnagi.2016.00119> (2016).
103. Sonnen, J. A. *et al.* Biomarkers for cognitive impairment and dementia in elderly people. *The Lancet Neurology* **7**, 704–714, [https://doi.org/10.1016/s1474-4422\(08\)70162-5](https://doi.org/10.1016/s1474-4422(08)70162-5) (2008).
104. Greicius, M. D. & Kimmel, D. L. Neuroimaging insights into network-based neurodegeneration. *Curr Opin Neurol* **25**, 727–734, <https://doi.org/10.1097/WCO.0b013e32835a26b3> (2012).
105. Hafkemeijer, A. *et al.* Resting state functional connectivity differences between behavioral variant frontotemporal dementia and Alzheimer's disease. *Frontiers in human neuroscience* **9**, 474, <https://doi.org/10.3389/fnhum.2015.00474> (2015).
106. Balthazar, M. L. *et al.* Neuropsychiatric symptoms in Alzheimer's disease are related to functional connectivity alterations in the salience network. *Human brain mapping* **35**, 1237–1246, <https://doi.org/10.1002/hbm.22248> (2014).
107. White, T. P., Joseph, V., Francis, S. T. & Liddle, P. F. Aberrant salience network (bilateral insula and anterior cingulate cortex) connectivity during information processing in schizophrenia. *Schizophrenia research* **123**, 105–115, <https://doi.org/10.1016/j.schres.2010.07.020> (2010).
108. Stam, C. J. & van Dijk, B. W. Synchronization likelihood: an unbiased measure of generalized synchronization in multivariate data sets. *Physica D* (2002).
109. Canuet, L. *et al.* Resting-state network disruption and APOE genotype in Alzheimer's disease: a lagged functional connectivity study. *PLoS one* **7**, e46289, <https://doi.org/10.1371/journal.pone.0046289> (2012).
110. Stam, C. J. *et al.* Magnetoencephalographic evaluation of resting-state functional connectivity in Alzheimer's disease. *NeuroImage* **32**, 1335–1344, <https://doi.org/10.1016/j.neuroimage.2006.05.033> (2006).
111. Papo, D., Zanin, M., Pineda-Pardo, J. A., Boccaletti, S. & Buldu, J. M. Functional brain networks: great expectations, hard times and the big leap forward. *Philosophical transactions of the Royal Society of London. Series B, Biological sciences* **369**, <https://doi.org/10.1098/rstb.2013.0525> (2014).
112. Shaw, L. M., Korecka, M., Clark, C. M., Lee, V. M. & Trojanowski, J. Q. Biomarkers of neurodegeneration for diagnosis and monitoring therapeutics. *Nature reviews. Drug discovery* **6**, 295–303, <https://doi.org/10.1038/nrd2176> (2007).
113. Dubois, J. & Adolphs, R. Building a Science of Individual Differences from fMRI. *Trends in cognitive sciences* **20**, 425–443, <https://doi.org/10.1016/j.tics.2016.03.014> (2016).

Acknowledgements

This work was supported by grants from CONICYT (National Commission for Scientific and Technological Research)/FONDECYT (National Fund for Scientific and Technological Development) Regular (1170010); CONICET (National Scientific and Technical Research Council); CONICYT/FONDAP (National Fund for Scientific and Technological Development) 15150012; the INECO (Institute of Cognitive Neurology) Foundation; PICT, Grant/ Award Number: 2017-1818 and 2017-1820; by the Inter-American Development Bank (IDB); by the Administrative Department of Science, Technology and Innovation (Colciencias) GRANT: 697-2014, 545-211; and the NHMRC (National Health and Medical Research Council).

Author Contributions

S.M. developed the algorithm, A.M.G., E.M., A.I. and L.S. the study concept and methodological design. Testing and data collection were performed by C.S., I.C.G., M.M., E.H., P.R. and D.M., while S.M., E.H. and S.C. analyzed the data and designed the figures. Results were interpreted by S.M., A.M.G., L.S., and A.I. The manuscript was written by S.M., with critical revisions from F.M., L.S., A.M.G., and A.I. All authors approved the final version of the manuscript for submission.

Additional Information

Supplementary information accompanies this paper at <https://doi.org/10.1038/s41598-018-29538-9>.

Competing Interests: The authors declare no competing interests.

Publisher's note: Springer Nature remains neutral with regard to jurisdictional claims in published maps and institutional affiliations.



Open Access This article is licensed under a Creative Commons Attribution 4.0 International License, which permits use, sharing, adaptation, distribution and reproduction in any medium or format, as long as you give appropriate credit to the original author(s) and the source, provide a link to the Creative Commons license, and indicate if changes were made. The images or other third party material in this article are included in the article's Creative Commons license, unless indicated otherwise in a credit line to the material. If material is not included in the article's Creative Commons license and your intended use is not permitted by statutory regulation or exceeds the permitted use, you will need to obtain permission directly from the copyright holder. To view a copy of this license, visit <http://creativecommons.org/licenses/by/4.0/>.

© The Author(s) 2018